Proceedings of the Sixth IASTED International Conference
EUROPEAN POWER AND ENERGY SYSTEMS
June 26–28, 2006, Rhodes, Greece

A POLE CANCELLATION STRATEGY FOR STABILISING A 3KW SOLAR POWER PLATFORM

J. T. Agee, Marie de Lazzer[1] and K. Yanev
Faculty of Engineering and Technology, University of Botswana
P. Bag 0061, Gaborone, BOTSWANA
agee@mopipi.ub.bw
1: Permanent address: Ecole Militaires de Saint Cyr, France

ABSTRACT
The paper investigates the dynamic performance of a locally designed 3KW solar power platform. A poorly damped dominant pole-pair (damping factor 0.0121) was found located near the origin of the s-plane of the transfer function of the open-loop platform system: causing overshoots of up to 96% and a long settling time of 105 seconds. A zero-pole cancelling controller was designed to replace these poorly-damped open-loop poles with a more stable dominant pole-pair. The controller improved the damping to 0.71, reduced the settling time to 2 seconds and the overshoot to 4.3%.

KEY WORDS
Solar power, Pole-Zero Cancellation, and Notch Filter Controller

1. INTRODUCTION

Botswana could be said to be a country blessed with abundant solar energy resource; having a mean solar day of 8.8 hours and 320 days of clear sunshine [1,2] in a year. It also experiences an excellent solar radiation intensity of 5.8 $KW.m^2$ [1]. Given that the country currently meets about 70% of her electricity needs through imports from the Southern African Power Pool (SAPP)[3,4,5], there is, therefore, a high incentive for locally developing technologies that could enhance the exploitation of this locally abundant energy resource (solar energy). More so that local investigations have shown that there is a good potential for use of solar power for rural enterprises in Botswana [2]. In a study recently undertaken at the Faculty of Engineering and Technology of the University of Botswana, it was found that solar installations with output power ranging from 1.0-3.0KW would be adequate for the range of enterprises found in most rural areas of the country [6]. A platform was subsequently designed for hosting ten 300W Shott solar panels (hence the total output of 3KW) [7]. Two additional Shell SQ 80 W solar panels [8] were provided for compensating for power losses as well as for supplying the D.C servomotor used for manoeuvring the platform in the East-West direction. The 3KW platform is shown in Figure 1; where the top view shows clearly the arrangement of the ten 300W solar panels together with the location of the two 80W panels, more to the centre of the platform. The view from under the platform shows both the frame work for supporting the solar panels and the link to the drive system for the daily east-to-west tracking of the direction of sunlight throughout the daylight period. The drive system consist of a d.c. motor linked to the platform through a gear train having a gear ratio of 800. The overall system forms a polar axis solar tracker system. This type of tracker is a particular case of a one-axis tracker and has been found from some field tests to yield 95% of the output of a dual axis tracker [9] while being comparatively much cheaper to acquire and less expensive to maintain. However, since our system is at this point an experimental one, the additional provision was made for manual control for the purposes of field experimentation in the Botswana environment. This manual provision for the seasonal adjustment of the longitudinal inclination of the platform is visible from Figure 1.b, where it appears like a knob on the stem supporting the platform.

As would be shown later in section three of this paper, simulations of the open-loop Solar Platform under a unit step change in the armature voltage of the d.c. drive system resulted in very large overshoots of the platform about its final rest position. There were also very large oscillations in the motor speed. In addition, the platform required nearly two minutes to settle down. On a practical platform, such large swings could result in the overstraining of associated mechanical structures. The long settling time also meant that the platform could not be guaranteed to track sunlight accurately, since it could be expected that the axis of the platform only comes to rest in a required direction long after the direction of the sun rays has significantly changed.

The rest of the paper reports the strategy that was used to improve the dynamic performance of the solar power platform. In the remaining parts of the paper, section two contains the modeling of the 3KW platform. The analysis of the dynamic performance of the open-loop platform system is shown in section three. Controller design and validation is contained in section four. Conclusions are included in section five. Acknowledgements and references conclude the paper.

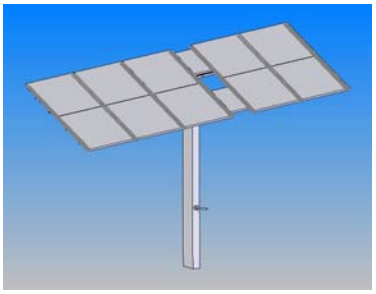

Figure 1.a: 3KW platform viewed from above

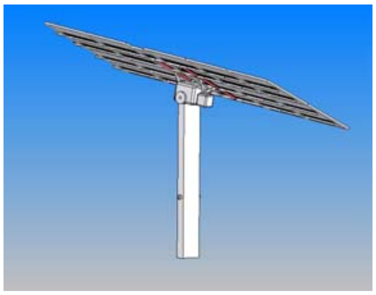

Figure 1.b: 3KW platform viewed from under

2. MODELLING OF THE 3 KW SOLAR TRACKER SYSTEM

The subsequent modeling presented in this section concerns the east-west motion of the platform. The block diagram representation of the platform in the east-west direction is shown in Figure 2.

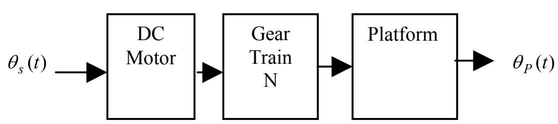

Figure 2: Block diagram of 3KW solar power platform

Where: $\theta s(t)$ is the instantaneous direction of sunlight and $\theta p(t)$ the instantaneous position of the platform.

Hence, the model of the solar tracker is the system of dynamic equations linking the separately excited dc motor to the platform through the gear train as derived in the sequel.

2.1 The Separately Excited DC Motor

The typical equivalent circuit arrangement for a separately excited DC motor is shown in Figure 3. An applied armature voltage e_a creates a armature current i_a given by [10]:

$$e_a = R_a i_a + L_a \frac{di_a}{dt} + K_b \frac{d\theta_m}{dt} \tag{1}$$

where $e_a(t)$: armature voltage (V); $i_a(t)$: armature

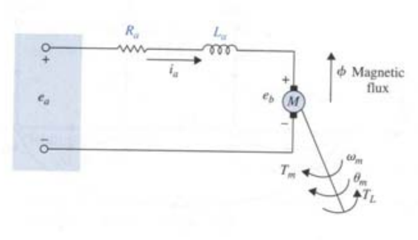

Figure 3: Schematic diagram of a separately excited DC motor.

current (A); R_a : armature resistance (Ω); L_a : armature inductance (H); K_b : back-emf constant (V/rad/s) and $\theta_m(t)$: rotor displacement (rad.). This current causes a torque $T_m = K_m i_a$ (2)

where $T_m(t)$ is torque(N.m.) and K_m the torque constant (N.m/A).

The torque of the DC motor is coupled to drive the platform through the motor shaft and a gear train. The torque causes an angular displacement of the rotor θ_m given by [10]

$$T_m = J_t \frac{d^2\theta_m}{dt^2} + B\frac{d\theta_m}{dt} + K\theta_m \tag{3}$$

where $J_t = J_m + N^2 J_l$ and J_m : moment of inertia of the motor ($kg.m^2$); J_l : moment of inertia of the load($kg.m^2$); N : gear-train ratio between motor and load; B : viscous-friction coefficient of the motor ($kg.m.s^{-1}$); K : spring constant ($kg.m^2.s^{-2}$). After taking the Laplace transform of equations (1)-(3), it is straightforward to obtain the open-loop transfer function for the system G(s)=θ_m(s)/E_a (s) as shown in equation (4).

$$G(s) = \frac{K_m / L_a J}{s^3 + \frac{(R_a J + L_a B)}{L_a J}s^2 + \frac{(R_a B + KL_a + K_b K_m)}{L_a J}s + \frac{R_a K}{L_a J}} \tag{4}$$

Note further that, the angular position of the platform θ_p is related to the motor angular position θ_m through the gear ratio: $\theta_p / \theta_m = N = 1/800$ (5)

The gear ratio was decided in comparing similar applications [10].

R_a=5Ω	L_a=0.003H	B=3.95.10^{-6} Kg.ms^{-1}
K_b=0.0636V/rad/s	K_m=0.00711 Kgm/A	K=0.01Kgm^{2}s^{-2}
J_M=7.72.10^{-6} Kg m^2	J_L=970Kgm^2	N=1/n=1/800

Table 1: System parameters.

The parameters of the open loop platform system are given in the Table 1. A substitution of these parameters in equation (4) results in the open-loop transfer function:

$$G(s) = \frac{1559.2}{s^3 + 1666.7s^2 + 109.87s + 10965} \quad (6)$$

In section three of the paper, the dynamic behaviour of this open loop system is investigated with the view to determining what controller would be most suitable for improving its dynamic performance.

3. ANALYSIS OF OPEN-LOOP PLATFORM SYSTEM

The analysis of the performance of the platform was realised using MATLAB. The following simulations were carried out.

3.1 Time-Domain Characterisation of the Open-Loop Platform System

The system was simulated for a unit step increase in the input voltage, The results are shown in Figure 4. The performance of the system, from Figure 4, could be summarized as in Table 2.

Settling time	105 Sec.
Peak Overshoot	96%
Steady State error	0.875%
Eigen Values	-1670, -0.031±j2.56

Table 2: Summary of the dynamic performance of the platform

It is evident from Figure 4 and the summary in Table 2 that the settling time of 105 sec. for the platform well exceeds one minute. This is too long and would not be suitable for the successful tracking of sunlight, since the direction of the sun rays is likely to change significantly before the platform settles down to the last command. Improvements in the settling time would be required. The peak overshoot is 96% of the final value. This is much higher than the maximum 17% overshoot acceptable in literature [10]. The maximum overshoot must be reduced. For a third order system, the damping ratio is not strictly defined [10]. However, the contribution of the root s_3=-1670 in the transient response is negligible. The complex pole-pair s_1, s_2=-0.031±j2.56 are the significant poles of the system. Their damping factor ξ is equal to 0.0121. This is much less than the optimum damping factor of ≈ 0.707 required for optimum plant performance [11]. An appropriate control strategy should enhance the damping of the system.

3.2 Frequency Analysis Of The Open Loop System

The frequency response of the system is shown in Figure 5. From the Bode plot, the Gain and Phase margins are read. The Gain margin is 40.86dB and the phase margin is 10.4 deg. While the gain margin seems adequate, the phase margin is too low; and is hence due for further improvements. More over, the Roots locus plots (Figure 5.b) show that even for very small increases in the forward gain of the system, the dominant pole pair cross the imaginary axis into the right half of the s-plane. It could be concluded that a control strategy that only increases the forward gain of the system, such as proportional control, would aid instability.

In the next section of the paper, we present the design of a controller that avoids increases in the forward gain of the system; and which replaces the existing dominant pole-pair of the plant with ones that have the optimum damping factor.

4. CONTROLLER DESIGN

The structure for the system with controller is shown in Figure 6. It consists of the following components:

4.1 The Sensor Circuit

The sensor circuit consist of two PV cells, used for determining the extent of misalignment of the platform with respect to the direction of sunlight. These cells are located equidistant on either side of the centre line along the North-South axis of the platform. To ensure that the cells intercept equal amount of solar radiation when the North-South line aligns with the direction of solar radiation, the cells are mounted on a line parallel to an imaginary east-west line that runs through the centre of the platform. Each cell generates a current proportional to the intensity of the incident light. This in turn depends on the orientation of the axis of the cell with respect to the direction of the sun rays. Whenever the platform is not exactly aligned to the direction of sunlight, the cells produce a differential current. Any difference in the short-circuit current of the two cells is sensed and amplified by an op-amp based current-to-voltage converter with a feedback resistor R_F to produce the error signal (in volts) for the controller. See, details in [6]

4.2 The Controller

4.2.1 Performance Specification

The controller was required to modify the response of the system in such a manner as to achieve the following performance specification:

- Settling time at 1% tolerance band = 2 seconds.
- Damping factor = 0.71

4.2.2 Controller Structure and Design

It has been explained earlier that, both the settling time and the damping of the platform system need improvement. Our solution was to use a controller whose transfer function zeros cancel the undesirable poles of G(s). Then, the poles of the controller can be placed to achieve the desired dynamic performance. Accordingly, the structure of the controller is specified to be the Notch filter with the following transfer function:

$$G_C(s) = \frac{K_1 s^2 + \alpha_1 s + \beta_1}{K_2 s^2 + \alpha_2 s + \beta_2} = \frac{N_1(s)}{D_1(s)} \tag{7}$$

The controller design entails the determination of the six coefficient $K_1, \alpha_1, \beta_1, K_2, \alpha_2$ and β_2. Note that the zeros of the controller are required to cancel the dominant pole-pair of the open-loop transfer function of the controlled system. Hence, $K_1 = 1$; $\alpha_1 = 0.062$ and $\beta_1 = 6.5546$. To determine K_2, α_2 and β_2 for the controller, consider the closed loop transfer function for the controlled system to obtain,

$$C(s) = \frac{NR_f G_C(s) G(s)}{1 + NR_f G_C(s) G(s)} \tag{8}$$

Now, $G_c(s)G(s)$ gives

$$\frac{(s+0.031-2.56j)(s+0.031+2.56j).1559.2}{D_1(s)(s+1670)(s+0.031-2.56j)(s+0.031+2.56j)} \text{ or}$$

$$G_C(s)G(s) = \frac{1559.2}{(K_2 s^2 + \alpha_2 s + \beta_2).(s+1670)}$$

Then,

$$C(s) = \frac{1559.2 NR_f}{(K_2 s^2 + \alpha_2 s + \beta_2).(s+1670) + 1559.2 NR_f} \tag{9}$$

Or C(s)=

$$\frac{1559.2 NR_f / K_2}{s^3 + (\frac{\alpha_2}{K_2} + 1670).s^2 + (\frac{\beta_2}{K_2} + 1670\frac{\alpha_2}{\beta_2})s + (1670\frac{\beta_2}{K_2} + 1559.2\frac{NR_f}{K_2})} \tag{10}$$

Also, for a damping factor of 0.71, the settling time is given by: $t_{s_{1\%}} = 4.6 / \xi\omega_n$ [10]. Thus, for a settling time of 2 seconds, we deduce $\omega_n = 3.24$ rad/s. The new dominant pole-pair is given by $s_{1,2} = -\xi\omega_n \pm \omega_n\sqrt{1-\xi^2}$ [10] yielding the dominant second-order factor $s^2 + 2\xi\omega_n + \omega_n{}^2$. With the third-pole of the closed-loop system situated at s= -d, we have the characteristic equation of the controlled system to be

$$s^3 + (d + 2\xi\omega_n)s^2 + (\omega_n^2 + 2\xi\omega_n d)s + d\omega_n^2 = 0 \tag{11}$$

Compare equations (10) and (11) to obtain the following relations:

$$\begin{aligned} 1670y + z &= d\omega_n^2 \\ \omega_n^2 + 2\xi\omega_n d &= y + 1670x \\ d + 2\xi\omega_n &= 1670 + x \end{aligned} \tag{12}$$

Where $x = \frac{\alpha_2}{K_2}, z = \frac{1.949 R_F}{K_2}; y = \frac{\beta_2}{K_2}$ (13)

The simultaneous solution of equation (12) yields for the un-damped natural frequency

$$\omega_n = 1670\xi \pm \sqrt{697225\xi^2 - 2788900 + z/\Delta} \tag{14}$$

$\Delta = d - 1670$

It becomes a matter of substitutions to verify that for the given settling time of 2 seconds and damping factor $\xi = 0.71$, equation (14) is satisfied for

$$z = 2893.664, \Delta = 0.0001 \tag{15}$$

and further that the closed loop pole s=-1670.0001, $\alpha_2 / K_2 = 4.6008; \beta_2 / K_2 = 8.7648$. By setting K_2=1, obtain the transfer function of the controller as:

$$G_C(s) = \frac{s^2 + 0.0620s + 6.5546}{s^2 + 4.6008s + 8.7648} \tag{16}$$

and $R_F = z / 1.949 = 1.485 K\Omega$

4.3 Performance of The Platform Equipped With Controller

The transfer function of the closed-loop system with controller becomes:

$$C(s) = \frac{2893.66}{s^3 + 1674s^2 + 7688s + 17505} \tag{17}$$

Both the transient response and the frequency response of the controlled system were simulated. The results are shown in Figure 7. It can be seen that, with the controller included, the system does not oscillate like it did before the introduction of the controller. The overshoot is 4.3%. Overshoot has been reduced by 95%, as compared to the case of the uncontrolled system. The damping factor is improved to 0.71. The settling time is now reduced to 2 seconds. The steady state error is only 0.01 deg. This is much better than for the uncontrolled system. In fact, the steady state error has been reduced by 99% . The system is stable. The gain margin is improved by 75% to about 73dB while the phase margin is now infinity. The peak armature current has been reduced by 25% from 0.2A to 0 0.16A . The peak torque required in the drive system increased from 1.5mN.m to 2.7mNm.

5. CONCLUSION

It could therefore be concluded that the pole cancellation control strategy improved significantly the dynamic performance of the 3KW solar power platform, improving the damping factor from 0.0121 to 0.71; reducing the settling time from 150 sec. to 2 sec. Peak overshoot of the rotor angular position was reduced by 95%. Both the gain margin and the phase margin were also substantially improved. The peak torque requirement however was doubled. The controller structure is simple and may be easily implemented. However, the design neglected nonlinear sensor characteristics which may restrict the usefulness of the control strategy presented here.

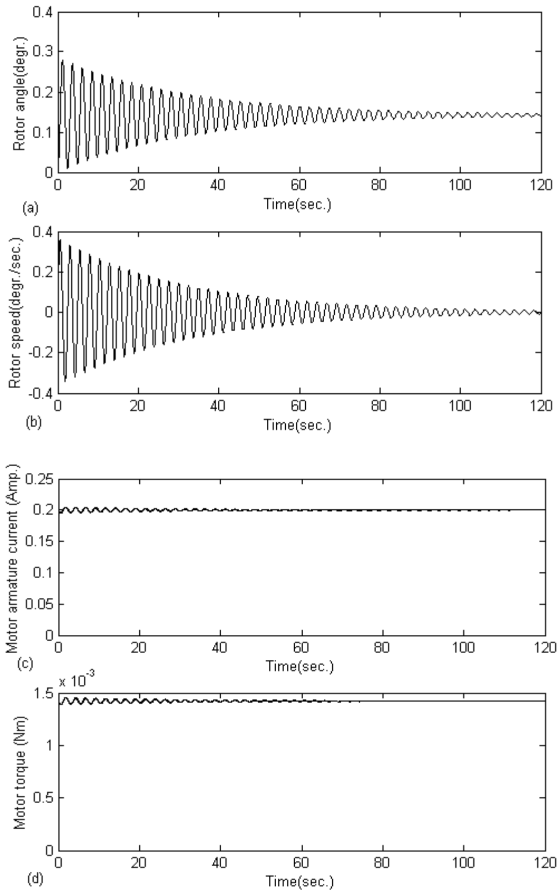

Figure 4: Dynamic response of solar platform without feedback control

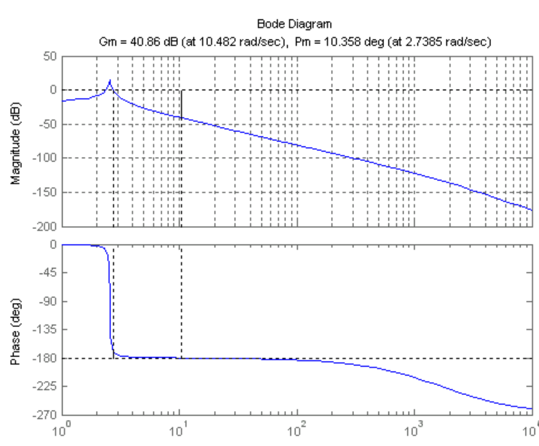

Figure 5.a: Bode plot of for uncontrolled plat form

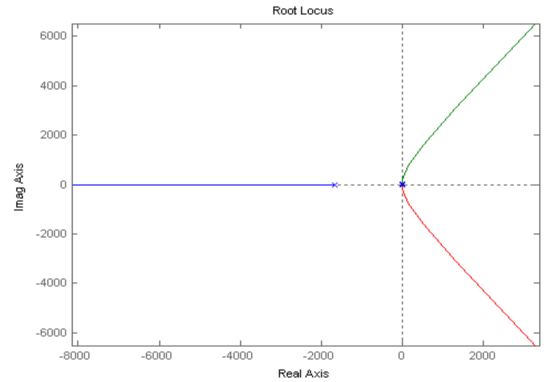

Figure 5.b: The root locus of uncontrolled platform

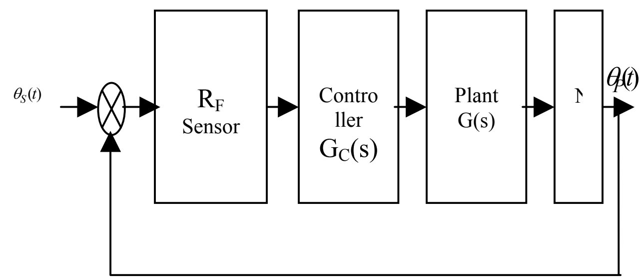

Figure 6: Block diagram of controlled solar platform

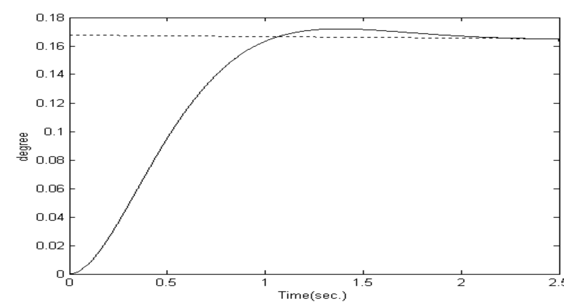

7.a: Rotor angle dynamics for the controlled platform system

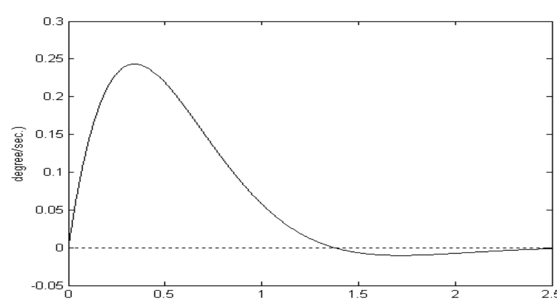

7.b: Rotor angular speeds for the controlled platform system

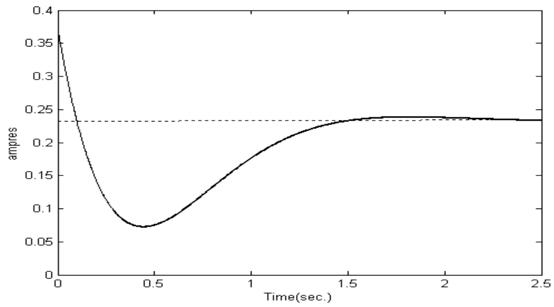

7.c: Armature current for the controlled platform system

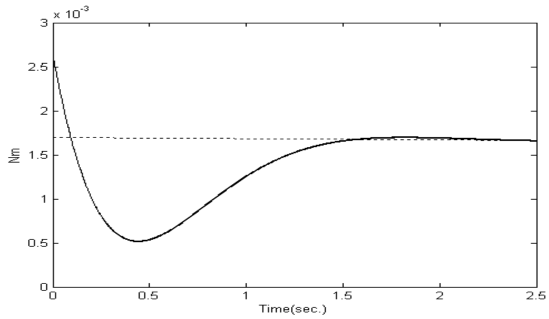

7.d: Motor torque for controlled platform system

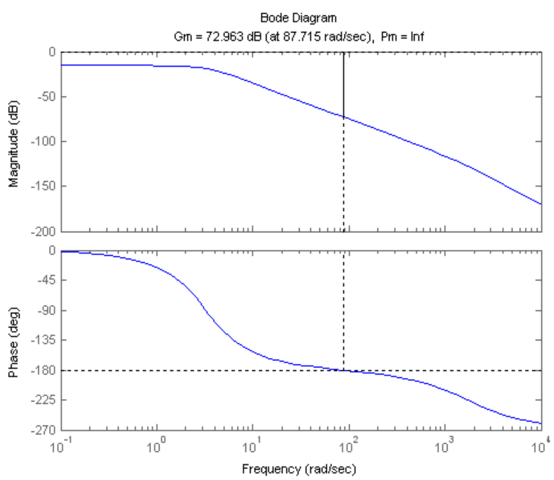

7e: Bode plot of controlled platform

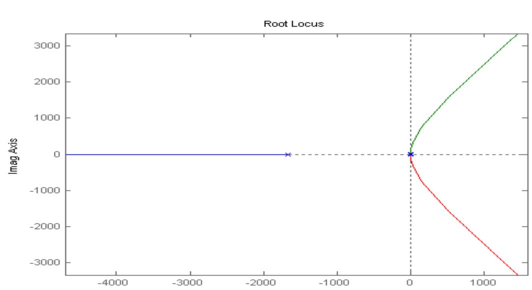

Figure 7f: Root locus of plot of controlled platform

ACKNOWLEDGEMENTS

Mister G. Jacobs, Director of Solar International Botswana, has proposed to make 14 solar panels available for testing the platform system. Botswana Technological centre (BOTEC) also supported this study in kind.

REFERENCES

[1] G. O. Anderson & M. H. Abkenari, Application of solar energy technology in Botswana. *Proc. IASTED Int. Conf. on Power and Energy Systems*. Las Vegas, Nevada, 1999, 141-150.

[2] Consultancy on Identifying and Overcoming Barriers to Widespread Adoption of Renewable Energy – Based Rural Electrification in Botswana: *Final report.* 2003.

[3] Botswana Power. http://www.wn.com/s/Botswana power. 2004.

[4] Southern Africa and the Southern African Development Community. http://www.eia.doe.gov /meu/cabs/sadc .hmtl. 2005.

[5] N. Matenge & V. Masilo, *Feasibility Study of Botswana Electricity Generation* (HND Project, *Power Point Presentation*, University of Botswana, 2004).

[6] Marie de Lazzer, *Positioning System for an Array of Solar Panels* M.Eng Thesis (Unpublished). University of Botswana and Ecoles de Saint Cyr, France, 2005).

[7] Alternative Energy Store, 300W Shott Solar panel specifications. http://shop.altenergystore.com , 2005.

[8] Shell SQ 80W solar panel specifications. http://www.shell.com, 2005.

[9] TRACSTAR (Small Power systems) Solar Tracking for Architects Source: http://www.pacificsites.com/ sps/trackforarc.html, 2006.

[10] B. C. Kuo & F. Golnaraghi, *Automatic Control Systems* (eight edition, John Wiley and Sons, Inc., 2003).

[11] N. S. Norman, *Control Systems Engineering* (John Willey and Sons, Inc. USA , 2004).